Available online at www.sciencedirect.com
ScienceDirect
Journal of Power Sources 162 (2006) 651–657
JOURNAL OF POWER SOURCES
www.elsevier.com/locate/jpowsour

Synthesis of $Li_3V_2(PO_4)_3$ with high performance by optimized solid-state synthesis routine

Peng Fu [a], Yanming Zhao [a,*], Youzhong Dong [a], Xiaoning An [b], Guopei Shen [c]

[a] *School of Physics, South China University of Technology, Guangzhou 510640, PR China*
[b] *School of Chemistry, South China University of Technology, Guangzhou 510640, PR China*
[c] *Guangzhou Hongsen Material Co., Ltd., Guangzhou 510760, PR China*

Received 7 March 2006; received in revised form 15 July 2006; accepted 19 July 2006
Available online 28 August 2006

Abstract

Monoclinic $Li_3V_2(PO_4)_3$ can be synthesized by solid-state reaction using either hydrogen or carbon as the reducing agent when sintering temperatures are higher than 800 °C. The initial capacity of $Li_3V_2(PO_4)_3$ synthesized using hydrogen as the reducing agent increases with increasing sintering temperature T and then for $T > 900$ °C decreases monotonically, and the sample synthesized at 900 °C present the highest initial capacity of 146.3 mAh g^{-1}, but exhibit poor cycle performance. The scanning electron microscope (SEM) images show that $Li_3V_2(PO_4)_3$ particles with small uniform particle size can be obtained at 900 °C. X-ray diffraction patterns of electrodes before and after cycling indicate that the capacity fading is not related to structure collapse. The carbon-coated $Li_3V_2(PO_4)_3$ (LVP/C) composites are synthesized by carbo-thermal reduction method at the optimized temperature of 900 °C. The LVP/C exhibit good cycle performance (137.5 mAh g^{-1} at 50th cycle under 1*C* rate, 94.6% of initial discharge capacity) and rate behavior (111.0 mAh g^{-1} under 5*C* rate for initial discharge) for the fully de-lithiated (3–4.8 V) samples. Our results suggest, based on the SEM images, that the good capacity retention and rate performance are owing to the nanometer size carbon webs coated the $Li_3V_2(PO_4)_3$ particles with both the greater specific surface area and the small uniform particle size.

Keywords: Lithium vanadium phosphates; $Li_3V_2(PO_4)_3$; Lithium battery; Carbon-coated $Li_3V_2(PO_4)_3$

1. Introduction

In recent years, the interesting in lithium rechargeable batteries in hybrid electric vehicles (HEVs) and electric vehicles (EVs) has been significantly increased [1–3]. The important factors for their application are low price, long cycle life, environmental safety, and high specific energy. The first commercial Li-ion rechargeable battery contains the layered materials $LiCoO_2$ and graphite as the cathode and anode, respectively. Although this battery is the current standard in many applications including cell phones and laptops, its slow charge and discharge rates, high cost and toxicity have prevented its using in large-scale applications [4,5].

In an intensive search for alternative materials, a wide variety of materials have been studied [6–8], and it is believed that there exist other compounds in the still unexploited reservoir of Li-compounds containing lithium elements and transition metal elements. Lithium transition metal phosphates, such as $LiFePO_4$ [7,8], have been the focus of candidate as cathode materials. Monoclinic lithium vanadium phosphate, $Li_3V_2(PO_4)_3$ (LVP), is a highly promising material proposed as a cathode for higher voltage lithium-ion batteries because it possesses good ion mobility, high reversible capacity and high operate voltage [9–12]. $Li_3V_2(PO_4)_3$ contains both mobile Li cations and redox-active metal sites housed within a rigid phosphate framework. The reversible cycling of all three lithiums from $Li_3V_2(PO_4)_3$ would correspond to a theoretical capacity of 197 mAh g^{-1} [13–17], this capacity is the highest for all phosphate which have been reported.

It was believed that in $Li_3V_2(PO_4)_3$ only two lithiums could be cycled reversibly until Huang et al. [16] and Saïdi et al. [17] demonstrated the extraction of the third Li from $Li_3V_2(PO_4)_3$. Morgan et al. [10] have used a combination of experimental and computational methods to characterize

* Corresponding author. Tel.: +86 20 87114370; fax: +86 20 85511266.
E-mail address: zhaoym@scut.edu.cn (Y. Zhao).

0378-7753/$ – see front matter © 2006 Elsevier B.V. All rights reserved.
doi:10.1016/j.jpowsour.2006.07.029

Table 1
Elemental composition of investigated samples (the oxygen content was calculated)

	Li (wt.%)	V (wt.%)	P (wt. %)	O_{cal} (wt.%)	C (wt.%)	Li:V:P (mole ratio)
$LI_3V_2(PO_4)_3$	5.11	24.82	22.86	47.21	–	2.97:1.98:3
$LI_3V_2(PO_4)_3$/C	4.61	22.33	20.57	42.49	10	2.98:1.98:3

the structure and electrochemical properties of $Li_xV_2(PO_4)_3$. However, to our knowledge no information has hitherto been obtained about the optimizing sintering temperatures as well as the structural information for the electrodes during the cycling on the electrochemical performance in $Li_3V_2(PO_4)_3$.

In this article, the preparation conditions on the properties of monoclinic $Li_3V_2(PO_4)_3$ as the cathodes materials have been investigated and, especially, both the influence of temperature and reducing agent/atmosphere on the single phase range, the morphology and the stability of the crystal structure during the charge and discharge when it serves as the cathodes materials were studied. The carbo-thermal reduction (CTR) method has been used to improving the cycle and rate performance, and the phenolic resin was added directly as carbon source. SEM images of pure and carbon-coated $Li_3V_2(PO_4)_3$ powders as well as the images of nanoporous carbon matrix obtained by using hydrochloric acid treatment to remove the $Li_3V_2(PO_4)_3$ were presented. The electrochemical performance of pure and carbon-coated $Li_3V_2(PO_4)_3$, and the XRD patterns of electrodes after performing different cycles were characterized in this article.

2. Experimental

The $Li_3V_2(PO_4)_3$ compounds were prepared using the solid-state reaction of V_2O_5, $NH_4H_2PO_4$, and Li_2CO_3. They were dispersed into acetone and then ball milled for 7 h in a planetary mill. After evaporating acetone, the mixture was first decomposed at 350 °C for 5 h to expel the gases. The resulting powders were then reground and transferred to an alumina boat. The $Li_3V_2(PO_4)_3$ was synthesized in a 93% Ar + 7% H_2 gas flow (50 ml min^{-1}) and sintered for 12 h at the temperatures ranging from 750 to 1050 °C. The carbon-coated $Li_3V_2(PO_4)_3$ (LVP/C) composites were prepared by CTR method where the carbon source, which was used as the reducing agent instead of H_2 gas, can be obtained by decomposing the phenolic resin. In this procedure the phenolic resin was added to the same raw materials as that for the preparation of $Li_3V_2(PO_4)_3$, after the initially calcined at 350 °C in N_2 and reground, LVP/C composite was synthesized at 900 °C for 12 h under flowing N_2 (50 ml min^{-1}) to yield a composite with 10% carbon in weight. The carbon content was verified by dissolved $Li_3V_2(PO_4)_3$ in hydrochloric acid and weighed the remains.

The phase identification of the product was carried out by XRD using a D/Max-2400 (Rigaku) diffractometer with Cu Kα radiation. The diffraction intensity data for Rietveld refinement analysis were collected by a MAX 18A-HF diffractometer with rotating anode, which had an 18 kW X-ray generator and Cu Kα radiation. A graphite monochromator was used for diffracted beams. A step scan mode was adopted with a scanning step of 0.02° and a sampling time of 3 s. Rietveld refinement was performed using the FullProf program to obtain the crystal structure parameters. Elemental composition of $Li_3V_2(PO_4)_3$ and LVP/C composite (Li, V, P) were determined by ICP-AES (inductively coupled plasma-atomic emission spectrometry) (TJA IRIS). SEM images were carried out with a JSM-6330F electron microscopy. The electrochemical characterization of $Li_3V_2(PO_4)_3$ powders as cathode of the two-electrode electrochemical cells were measured using an automatic battery tester system (Land®, China). The cathode of the two-electrode electrochemical cells were fabricated by blending the prepared powder with acetylene black and polyvinylidiene fluoride (PVDF) binder in a weight ratio of 75:15:10 in *N*-methyl-2-pyrrolidone (NMP). For the LVP/C composite as cathode, the weight ratio was 85:5:10. The obtained slurry was coated on Al foil, dried at 50 °C for 24 h and pressed (5 MPa), respectively. The electrodes fabricated were dried again at 80 °C for 12 h in vacuum and cut into 1 cm × 1 cm in size where about 5 mg of active materials was hold on it. Two-electrode electrochemical cells were assembled in a Mikrouna glove box filled with high-purity argon, where the lithium metal foil were used as anode, Celgard® 2320 as separator, and 1 M $LiPF_6$ in EC:DMC (1:1 vol.%) were used as an electrolyte. The electrochemical capacity measurements were performed in the voltage range between 3.0 and 4.3, 3.0–4.5 and 3.0–4.8 V, and the electrochemical capacity of samples was evaluated on the active materials.

3. Results and discussion

In order to verify the purity of the compound studied here, the elemental analysis has been performed. As shown in Table 1, according to element analysis results from ICP-AES, Li, V, and P contents are in the line with those expected for a stoichiometry of $Li_3V_2(PO_4)_3$. Fig. 1 shows the XRD profiles of $Li_3V_2(PO_4)_3$ synthesized at 750–950 °C. As shown in Fig. 1a and b, when the

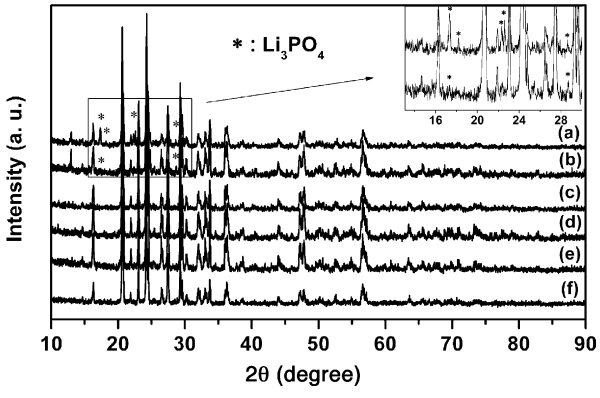

Fig. 1. X-ray diffraction profiles of $Li_3V_2(PO_4)_3$ sintered at (a) 750 °C; (b) 800 °C; (c) 850 °C; (d) 900 °C; (e) 950 °C and (f) 900 °C with carbon coated.

temperatures ranging between 750 and 800 °C, $Li_3V_2(PO_4)_3$ is the dominate phase, but the impurity phase Li_3PO_4 exists obviously. When the temperature was higher than 850 °C, single-phase $Li_3V_2(PO_4)_3$ with monoclinic structure were obtained (Fig. 1c–e).

Since small amount impurities affect the electrochemical properties, the more precise XRD patterns should be provided. Fig. 2 shows the Rietveld refinement of the powder X-ray diffraction data of $Li_3V_2(PO_4)_3$ compound sintered at 900 °C, and a space group of $P2_1/n$ was chosen as the refinement model. The weighted factor R_{wp} is 10.7%. The cell parameters with $a = 8.6079(5)$ Å, $b = 8.5957(2)$ Å, $c = 12.0400(3)$ Å and $\beta = 90.5859(9)°$ obtained from the result of the Rietveld refinement agree well with the values reported previously [9]. The reasonably small R_{wp} factor (~10.7%) suggests that single-phase $Li_3V_2(PO_4)_3$ can be obtained under our experimental process, and no impurity phases can be detected under the resolution of our X-ray diffractometer. In the inset of Fig. 2, the structure of $Li_3V_2(PO_4)_3$ based on the crystal structure parameters obtained from Rietveld refinement is presented. In this monoclinic structure, each unit cell contains four chemical formula units of $Li_3V_2(PO_4)_3$, all the Li, V, P, and O atoms occupy Wyckoff position 4e with different coordinates. The atomic parameters are given in Table 2. The monoclinic structure comprises a framework of metal octahedra and phosphate tetrahedra sharing oxygen vertices. Each VO_6 octahedron is surrounded by six PO_4 tetrahedra, whereas each PO_4 tetrahedron is surrounded with four VO_6 octahedra. This configuration forms a three-dimensional network. The electric charge carriers, lithium ions, are located in the cavities within the framework. The three crystallographic independent Li sites in $Li_3V_2(PO_4)_3$: Li_1, Li_2, and Li_3 are 4-, 5- and 5-coordinate, respectively. Three four-fold crystallographic positions exist for the Li atoms leading to twelve lithium positions within the unit cell. The three-dimensional structure allows for reversible extraction of all three lithium ions from the monoclinic vanadium phosphate at slow, and even at very fast rates [16].

Table 2
Atomic sites (number of positions and Wyckoff notation) and coordinates x, y, z (in units of lattice constants $a = 8.6079(5)$ Å; $b = 8.5957(2)$ Å; $c = 12.0400(3)$ Å and $\beta = 90.5859(9)°$) for $Li_3V_2(PO_4)_3$

Atom	x	y	z	N
Li_1 (4e)	0.2174(2)	0.8302(5)	0.1438(5)	4
Li_2 (4e)	0.9260(7)	0.3092(7)	0.2508(1)	4
Li_3 (4e)	0.5912(3)	0.4296(3)	0.1915(5)	4
V_1 (4e)	0.2493(1)	0.4628(9)	0.1100(7)	4
V_2 (4e)	0.7508(2)	0.4718(6)	0.3909(6)	4
P_1 (4e)	0.1070(7)	0.1027(6)	0.1472(4)	4
P_2 (4e)	0.6062(4)	0.1178(5)	0.3536(9)	4
P_3 (4e)	0.0379(4)	0.2498(2)	0.4924(8)	4
O_1 (4e)	0.9181(1)	0.1164(9)	0.1512(9)	4
O_2 (4e)	0.1497(4)	0.9730(8)	0.2391(1)	4
O_3 (4e)	0.1707(4)	0.0491(7)	0.0415(7)	4
O_4 (4e)	0.1641(9)	0.2691(3)	0.1891(1)	4
O_5 (4e)	0.4310(4)	0.0892(3)	0.3332(1)	4
O_6 (4e)	0.6949(5)	0.0011(4)	0.2793(9)	4
O_7 (4e)	0.6469(7)	0.0888(1)	0.4793(3)	4
O_8 (4e)	0.6437(3)	0.2875(1)	0.3131(2)	4
O_9 (4e)	0.9540(9)	0.1283(5)	0.5672(5)	4
O_{10} (4e)	0.9295(1)	0.3212(3)	0.4042(9)	4
O_{11} (4e)	0.1757(1)	0.1690(3)	0.4222(1)	4
O_{12} (4e)	0.1181(2)	0.3584(1)	0.5746(7)	4

Our experimental results show that the cathode performance depend strongly on the sintering temperature although the single phase $Li_3V_2(PO_4)_3$ can be obtained at the temperatures higher than 850 °C. The initial capacity of single phase $Li_3V_2(PO_4)_3$ as cathode as a function of sintering temperature is represented in Fig. 3. The initial capacity of $Li_3V_2(PO_4)_3$ compounds shows an interesting sintering temperature dependence. The initial capacity increases with increasing sintering temperature T and then for $T > 900$ °C decreases monotonically. The sample synthesized at 900 °C exhibit the highest initial capacity of 146.3 mAh g^{-1}. In order to elucidate what happens for the morphology of the powders obtained at the temperatures higher than 800 °C, Fig. 4a–d exhibit the SEM images for samples sintered at the different

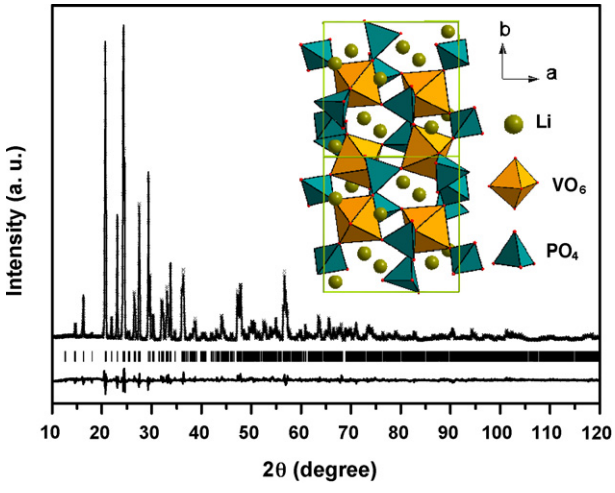

Fig. 2. XRD refinement results of $Li_3V_2(PO_4)_3$ sintered at 900 °C. The observed data are indicated by crosses and the calculated profile is the continuous line overlaying them. The different between the experimental and calculated values is shown as continuous line at the bottom. Inset shows the crystal structure of $Li_3V_2(PO_4)_3$.

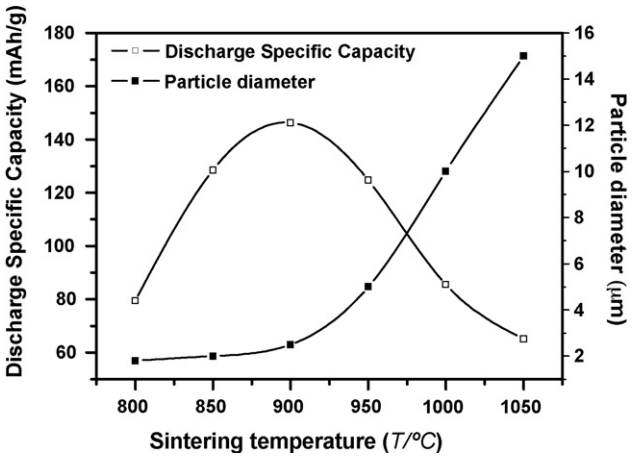

Fig. 3. Change in capacity (first discharge at 1C rate between 3 and 4.8 V) and particle size of $Li_3V_2(PO_4)_3$ sintered at six different temperatures.

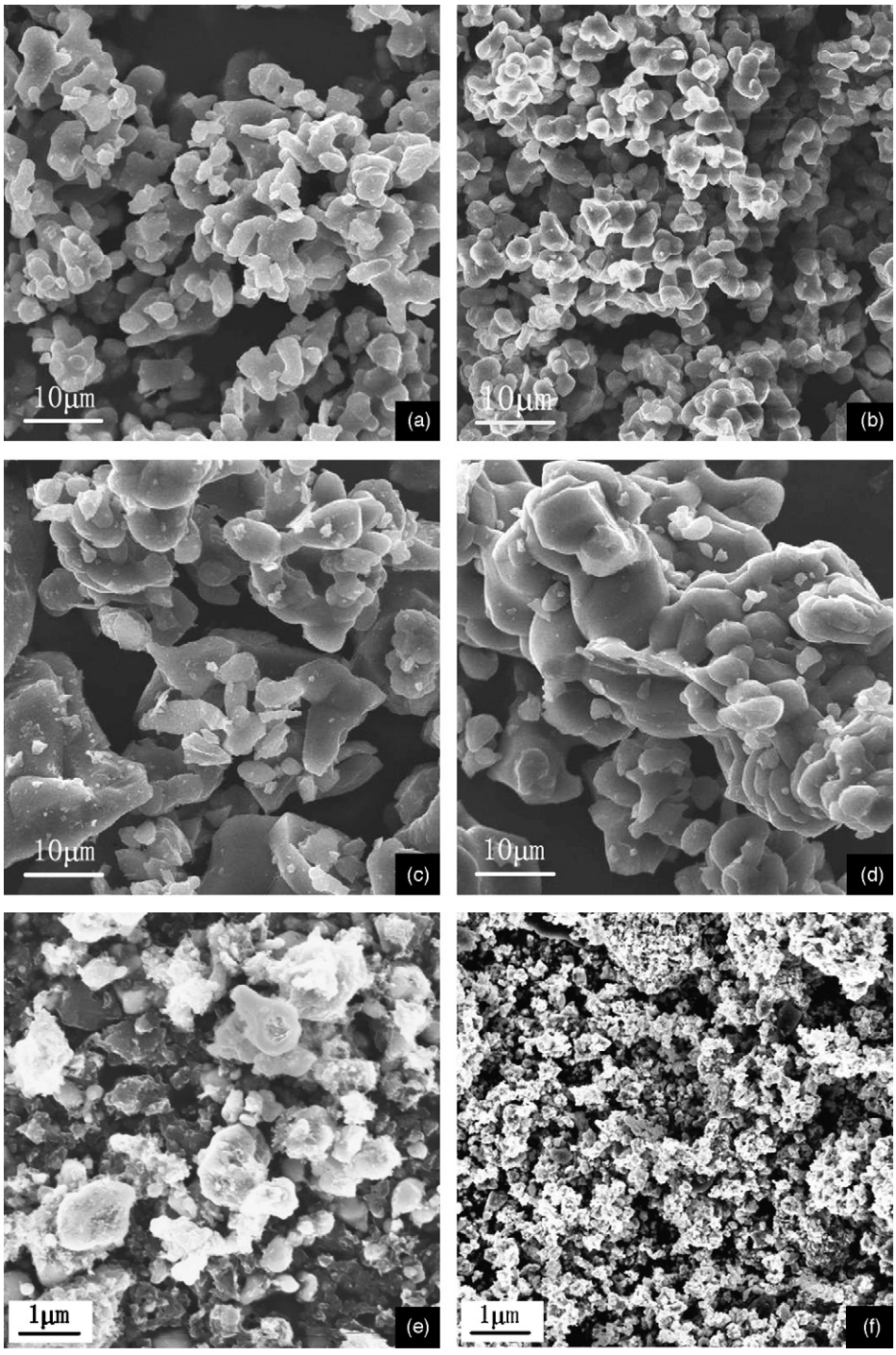

Fig. 4. SEM images of pure $Li_3V_2(PO_4)_3$ sintered at (a) 850 °C; (b) 900 °C; (c) 950 °C; (d) 1000 °C and (e) LVP/C, (f) after acid treatment to remove the $Li_3V_2(PO_4)_3$ showing the nanoporous carbon matrix.

temperatures, and the dependence of the particle size obtained from Fig. 4 on sintering temperatures is shown in Fig. 3.

From Fig. 4a we can see that there are insufficient sintering for the samples prepared at lower temperature ($T < 900$ °C). The small non-uniform particles which are agglomerated with the particle size of about 1–2 μm can also be observed in Figs. 4a and 3, respectively, where the abundance of grain-boundary leads to poor connection of $Li_3V_2(PO_4)_3$ particles, which may be responsible for the lower initial capacity than that for the samples prepared at 900 °C. In contrast, higher temperature ($T > 900$ °C) preparation caused the abrupt particles growth (shown in Fig. 3) with a smooth surface (shown in Fig. 4c–d), and correspondingly, resulting in an abrupt drop in capacity.

Although monoclinic $Li_3V_2(PO_4)_3$ has been stated as a high rate cathode, the fast-ion conducting Nasicon structure results in reversible extraction of all three lithium ions from the host materials even at fast rate [16], in this paper, we found that the morphology and specific surface area of obtained particles still

have the notable effect on the cycle performance of the products. The samples have the smaller uniform particle size and relative higher specific surface area presented the better electrochemical performance. In particles with a larger diameter and a relative lower specific area, considering its inferior electronic conductivity, the electronics have to diffuse over greater distance between the surface and center during lithium insertion or extraction, and the active materials near the center of particle contributes very little to the charge/discharge reaction [5]. Our experimental results suggest that the better performance can be obtained with optimizing the powder characteristic at a moderate temperature of 900 °C. The small uniform particles with the diameter of about 2 μm (Fig. 4b), which have a relative larger specific area, can bring on the better performance exhibits. The abrupt increase of particle size at the temperatures higher than 900 °C can be responsible for the decreasing of the initial capacity monotonically when the sintering temperatures are higher than 900 °C.

Although the sample synthesized at 900 °C has the highest initial capacity, its cycle performance is not remarkable. The capacity of $Li_3V_2(PO_4)_3$ synthesized at 900 °C decreases rapidly, from 146.3 mAh g^{-1} of the first cycle to 110.3 mAh g^{-1} in the 50th cycle (75.4% of the initial capacity) at 1*C* rate, and Fig. 5a shows clearly the capacity fading of $Li_3V_2(PO_4)_3$.

In order to understand the observed electrochemical behaviors (see in Fig. 5a), the X-ray diffraction patterns of electrodes before cycling and after 10, 20 and 50 cycles were compared. As shown in Fig. 6, the variations of peaks position, peak sharp and relative intensity of the X-ray diffraction patterns are not distinguishable before and after cycling. This observation indicates that it is difficult to relate the capacity fading with the structural collapse during charge/discharge process, and when combined the SEM images shown in Fig. 4 with the electrochemical behaviors (see in Fig. 5), we can conclude that the reasons for capacity fading can be attributed to the relative large crystallite size and, especially the poor electric contact in pure $Li_3V_2(PO_4)_3$ powders.

In order to control the particle size of $Li_3V_2(PO_4)_3$ and enhance its electronic conductivity, the carbon-coated

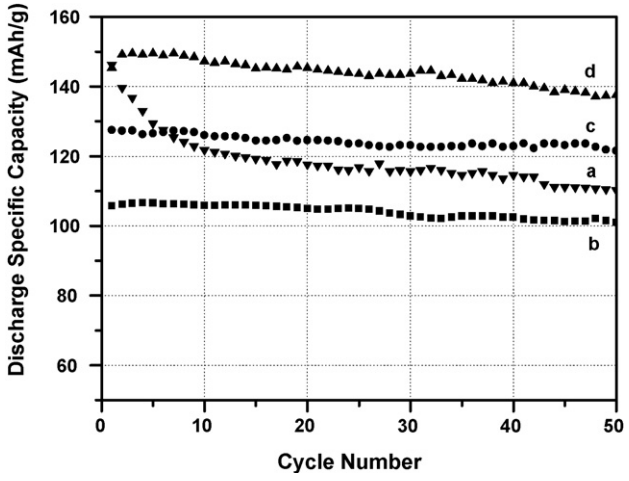

Fig. 5. Cycle performance of (a) pure $Li_3V_2(PO_4)_3$ between 3 and 4.8 V, (b) LVP/C between 3 and 4.3 V; (c) 3–4.5 V; (d) 3–4.8 V at 1*C* rate.

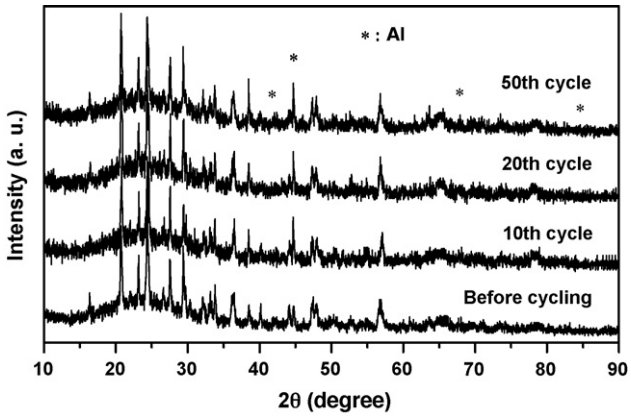

Fig. 6. The XRD patterns of $Li_3V_2(PO_4)_3$ as electrodes in different cycles.

$Li_3V_2(PO_4)_3$ composite was synthesized by CTR method using phenolic resin as carbon source, and according to the previous results shown in Fig. 3, the temperature of 900 °C was chosen as the right sintering temperature for the thereafter studies. The phase identification of LVP/C was carried out from the XRD patterns and, as shown in Fig. 1f, there is a good correspondence of the X-ray diffractions patterns for the LVP/C and the pure $Li_3V_2(PO_4)_3$. The amount of Li, V, P and O is also almost equal to the preset value according to ICP-AES results, as shown in Table 1. As shown in Fig. 1, no peaks shift are observed in Fig. 1f indicate that carbon coating does not affect the monoclinic structure of $Li_3V_2(PO_4)_3$, while the lower peak intensity of LVP/C than that of pure $Li_3V_2(PO_4)_3$ may be due to the addition of the amorphous phase carbon.

The cycle performance of LVP/C composite measured at room temperature is shown in Fig. 5b–d. The voltage cut-offs were chosen according to the work of Yin et al. [14] and Saïdi et al. [15]. Charge–discharge performances were measured between 3.0 and 4.3, 3.0–4.5 and 3.0–4.8 V so as to remove the equivalent of 2, 2.5 and 3 lithiums. The LVP/C samples exhibit a good capacity retention without obviously capacity fading after 50 cycles and, as shown in Fig. 5, a sustained cycling behaviors (110, 130 and 150 mAh g^{-1} specific capacities for 4.3, 4.5 and 4.8 V voltage cut-offs at 1*C* rate, respectively) can be obtained. At the 50th cycle, the discharge capacity between 3.0 and 4.3 V, 3.0–4.5 V and 3.0–4.8 V is 101.5 mAh g^{-1} (95.9% of initial capacity), 121.6 mAh g^{-1} (95.4% of initial capacity) and 137.5 mAh g^{-1} (94.6% of initial capacity), respectively.

It is well known that the rate capability is very important if commercially viable systems are to be developed. In this context, rate capability refers to the ability of an electrode material to retain its capacity when discharged in different rates. LVP/C shows a good rate performance even at 5*C* rate as shown in Fig. 7, where the rate performances were measured between 3.0–4.3 and 3.0–4.8 V. From Fig. 7 we can see that LVP/C has an initial discharge capacity of 161.9, 152.9, 145.3, 130.7 and 111.0 mAh g^{-1} between 3 and 4.8 V under 0.2, 0.5, 1, 2 and 5 *C* rate, respectively. The initial discharge capacity between 3 and 4.3 V under 0.2, 0.5, 1, 2 and 5 *C* rate is 115.8, 109.2, 105.9, 97.2 and 73.2 mAh g^{-1}, respectively.

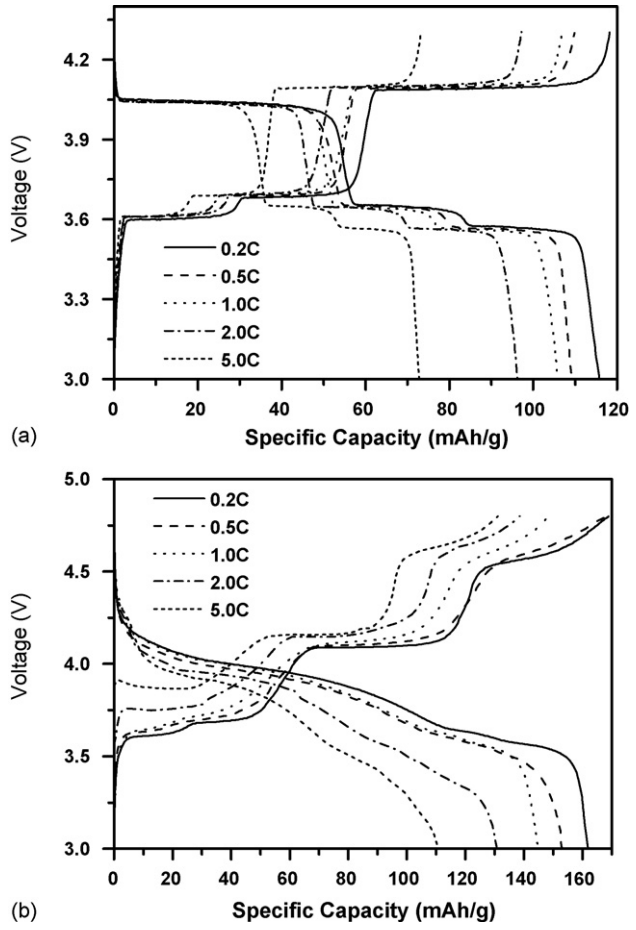

Fig. 7. Rate performance (second discharge) of LVP/C between (a) 3.0–4.3 V and (b) 3.0–4.8 V.

In order to explain why the carbon-coated $Li_3V_2(PO_4)_3$ have the better cycle and rate performance, the SEM images shown in Fig. 4e–f were compared carefully. From SEM image shown in Fig. 4e, we can see that the average particle size is around 0.5 μm for LVP/C composite, which is much smaller than that of about 2 μm for pure (uncoated) $Li_3V_2(PO_4)_3$. Because it is hard to discern carbon from $Li_3V_2(PO_4)_3$ powders, we dissolved the $Li_3V_2(PO_4)_3$ composite in hydrochloric acid, and as shown in Fig. 4f, our observed results reveal the presence of a nano-structured carbon web in which the crystallites had been embedded. The SEM images suggest that the web resembles a thin-walled carbon sponge with nanoscale dimensions on the order of 100 nm, which percolated throughout with interconnected voids that house the $Li_3V_2(PO_4)_3$ crystallites. The carbon sponge percolative transport through the $Li_3V_2(PO_4)_3$ crystallites interspaces is responsible for the electronic properties of the LVP/C composite. It is expected that this type of composite would be very effective in enhancing the electronic conductivity of $Li_3V_2(PO_4)_3$. This relatively large capacity and high rate capacity of LVP/C may be attributed to coating the nanometer size carbon webs on the $Li_3V_2(PO_4)_3$ particles with the greater specific surface area and the uniform small particle size of 0.5 μm.

4. Conclusion

Single phase monoclinic samples of $Li_3V_2(PO_4)_3$ can be synthesized by direct solid-state reaction using either hydrogen or carbon as the reducing agent when the sintered temperatures are higher than 850 °C. The initial capacity of $Li_3V_2(PO_4)_3$ synthesized using hydrogen as the reducing agent increases with increasing sintering temperature T and then for $T > 900$ °C decreases monotonically, and the sample synthesized at 900 °C exhibit the highest initial capacity of 146.3 mAh g^{-1}, but exhibit poor cycle performance. The SEM images show that the synthesis temperatures play an important role on the crystallite size and the uniformity of its surface. The XRD patterns of electrodes before and after cycling indicate that the capacity fading is not related to structure collapse. The carbon-coated $Li_3V_2(PO_4)_3$ composites are synthesized by CTR method. The LVP/C composites exhibit good cycle performance (137.5 mAh g^{-1} at 50th cycle under 1C rate, 94.6% of initial discharge capacity) and rate behavior (130.7 mAh g^{-1} under 2C rate and 111.0 mAh g^{-1} under 5C rate for initial discharge) for the fully de-lithiated (3–4.8 V) samples. Based on the SEM images of LVP/C, the good capacity retention and rate performance are owing to the coexistence of $Li_3V_2(PO_4)_3$ particles with both the greater specific surface area and the uniform small particle size and the carbon sponge phase in a broad range, which leads to the minimum volume fractions of grain-boundary and, thereby, the maximum "connection" of $Li_3V_2(PO_4)_3$ particles.

Acknowledgements

This work was funded by NSFC Grant (No. 50472055 and No. 10274048) supported through NSFC Committee of China and Science and Technology Foundation supported through the Science and Technology Department of Guangdong Province respectively.

References

[1] M. Winter, R.J. Brodd, Chem. Rev. 104 (2004) 4245–4269.
[2] M.S. Whittingham, Chem. Rev. 104 (2004) 4271–4301.
[3] P.S. Herle, B. Ellis, N. Coombs, L.F. Nazar, Nat. Mater. 3 (2004) 147–152.
[4] A.K. Padhi, K.S. Nanjundaswamy, J.B. Goodenough, J. Electrochem. Soc. 144 (1997) 1188–1194.
[5] A.S. Andersson, J.O. Thomas, J. Power Sources 97/98 (2001) 498–502.
[6] M. Higuchi, K. Katayama, Y. Azuma, M. Yukawa, M. Suhara, J. Power Sources 119–121 (2003) 258.
[7] A. Yamada, S.C. Chung, K. Hinokuma, J. Electrochem. Soc. 148 (2001) A224–A229.
[8] S.-Y. Chung, J.T. Bloking, Y.-M. Chiang, Nat. Mater. 1 (2002) 123–128.
[9] S.-C. Yin, H. Grondey, P. Strobel, M. Anne, L.F. Nazar, J. Am. Chem. Soc. 125 (2003) 10402–10411.
[10] D. Morgan, G. Ceder, M.Y. Saidi, J. Swoyer, H. Huang, G. Adamson, Chem. Mater. 14 (2002) 4684–4693.
[11] J. Gaubicher, C. Wurm, G. Goward, C. Masquelier, L. Nazar, Chem. Mater. 12 (2000) 3240–3242.
[12] M. Sato, H. Ohkawa, K. yoshida, M. Saito, K. Uematsu, K. Toda, Solid State Ionics 135 (2000) 137–142.
[13] S.-C. Yin, P.S. Strobel, H. Grondey, L.F. Nazar, Chem. Mater. 16 (2004) 1456–1465.

[14] S.-C. Yin, H. Grondey, P. Strobel, H. Huang, L.F. Nazar, J. Am. Chem. Soc. 125 (2003) 326–327.
[15] M.Y. Saïdi, J. Barker, H. Huang, J.L. Swoyer, G. Adamson, J. Power Sources 119–121 (2003) 266–272.
[16] H. Huang, S.-C. Yin, T. Kerr, N. Taylor, L.F. Nazar, Adv. Mater. 14 (2002) 1525–1528.
[17] M.Y. Saïdi, J. Barker, H. Huang, J.L. Swoyer, G. Adamson, Electrochem. Solid State Lett. 5 (2002) A149–A151.